Journal for ImmunoTherapy of Cancer

Targeting CD96 overcomes PD-1 blockade resistance by enhancing CD8+ TIL function in cervical cancer

Yumeng Wang ,[1,2] Congwen Wang,[2,3] Junjun Qiu,[1,2] Xinyu Qu,[1,2] Jing Peng,[2,3] Chong Lu,[2,3] Meng Zhang,[2,3] Mingxing Zhang,[2,3] Xingling Qi,[2,3] Guiling Li,[2,3] Keqin Hua[1,2]

To cite: Wang Y, Wang C, Qiu J, *et al*. Targeting CD96 overcomes PD-1 blockade resistance by enhancing CD8+ TIL function in cervical cancer. *Journal for ImmunoTherapy of Cancer* 2022;**10**:e003667. doi:10.1136/jitc-2021-003667

► Additional supplemental material is published online only. To view, please visit the journal online (http://dx.doi.org/10.1136/jitc-2021-003667).

GL and KH contributed equally.

YW, CW and JQ are joint first authors.

Accepted 16 February 2022

[1]Department of Gynecology, Obstetrics and Gynecology Hospital of Fudan University, Shanghai, China
[2]Shanghai Key Laboratory of Female Reproductive Endocrine Related Diseases, Obstetrics and Gynecology Hospital of Fudan University, Shanghai, China
[3]Department of Integration of Western and Traditional Medicine, Obstetrics and Gynecology Hospital of Fudan University, Shanghai, China

Correspondence to
Professor Guiling Li;
guilingli@fudan.edu.cn

Professor Keqin Hua;
huakeqin@fudan.edu.cn

ABSTRACT

Background Novel therapies are needed to treat recurrent and advanced cervical cancer (CC), as their prognosis remains very poor. Although therapies targeting the programmed cell death protein 1 (PD-1) pathway have been approved for CC, a large subset of patients exhibit innate resistance. Using checkpoint inhibitors in combination could enhance their efficacy.

Methods Blood samples, tumor specimens, and peritumorous (PT) tissues were obtained from patients with CC. The inhibitory receptor expression and phenotypical analysis of CD8+ T cells in CC specimens were analyzed by flow cytometry. The ligands of CD96 expressed by tumor cells were measured by immunohistochemistry and immunofluorescence. Sensitivity to pembrolizumab was evaluated by an ex vivo treatment assay based on the single-cell culture of CC specimens. The efficacies of PD-1 and/or CD96 blockades were explored using an ex vivo treatment assay and an human papillomavirus-positive TC-1 xenograft mouse model in vivo.

Results We found that CD96 expression was elevated on CD8+ tumor-infiltrating lymphocytes (TILs) from patients with CC who were insensitive to the PD-1 blockade. These CD96-expressing CD8+ TILs often coexpressed PD-1. The ratio of the CD96+CD8+/CD96−CD8+ T-cell gene signature from the scRNA-seq data was significantly associated with the poor survival of patients with cervical squamous cell carcinoma and endocervical adenocarcinoma. The costimulatory receptor CD226, which competes with CD96, was downregulated in tumors compared with blood and PT tissue. CD96 and T-cell immunoreceptor with Ig and ITIM domains (TIGIT) were upregulated on intratumoral CD8+ T cells. The CD226/CD96/TIGIT signaling ligands were widely expressed in CC tumor tissues. Phenotypical profiling showed that PD-1+CD96+CD8+ TILs exhibited a terminally exhausted effector phenotype with high levels of T-cell immunoglobulin mucin receptor 3 (TIM-3) and granzyme B (GZMB) and extremely low levels of proinflammatory cytokines and cytotoxic molecules. PD-1+CD96 cells exhibited a precursor exhausted phenotype with TCF-1 positivity. CD96 was further upregulated by CD8+ TILs on PD-1 blockade. Treatment with the CD96 blockade significantly enhanced the PD-1 blockade to blunt tumor growth and improve the function of CD8+ TILs in both mouse and CC specimen models.

Conclusions Our findings showed that CD96 and PD-1 cooperatively and negatively regulate the function of CD8+ TILs, and CD96 blockade has promise for use in combination with PD-1 blockade for the treatment of CC.

INTRODUCTION

Despite improvements in screening and prophylactic vaccination, cervical cancer (CC) remains one of the most common malignancies among women, with an estimated 57 000 new cases and approximately 31 100 deaths in women worldwide.[1] The current first-line strategy for CC consists of surgery, chemotherapy or radiotherapy for locally advanced disease, and platinum-based chemotherapy with or without the anti-vascular endothelial growth factor (VEGF) drug bevacizumab for advanced disease.[2 3] These treatments have reduced the mortality rate of CC, but their effectiveness is now reaching a plateau. In particular, the survival outcomes of patients with recurrent or advanced CC are poor, with a median overall survival (OS) of approximately 17 months and an estimated 5-year survival rate of approximately 17%.[4] The life expectancy after CC recurrence is less than 2 years and is even shorter if subsequent chemotherapies fail.

In the past decade, therapies targeting the immune checkpoint molecule programmed cell death protein 1 (PD-1) and its ligand, PD-L1, have revolutionized cancer treatment. Based on a phase II study in which 11 (14%) of 77 patients with PD-L1-positive recurrent or advanced CC who received one or more lines of chemotherapy had an objective response to pembrolizumab,[5] the US Food and Drug Administration granted accelerated approval of pembrolizumab as a second-line treatment for patients who were PD-L1 positive with disease progression after chemotherapy. Despite the tremendous clinical successes of anti-PD-1/PD-L1

monoclonal antibodies in some cancer types, the overall response rate to checkpoint immunotherapy remains modest for most cancers (12.46% in 2018 among US patients).[6] Even though CC meets most criteria regarding immune checkpoint blockade (ICB) suitability, from its robust PD-1/PD-L1 expression and a T cell-inflammatory phenotype to the mutational load and immunogenicity of human papillomavirus-positive tumors, patients with CC exhibit low response rates of 4%–26.3% to current ICBs, including pembrolizumab.[5 7–9] While the use of ICB for the treatment of CC is generally supported, the consensus is that it has not reached its full potential. Therefore, for CC and other tumors, combinational therapies present a tantalizing alternative to the standard of care for overcoming resistance and improving efficacies of future therapies.[10]

To identify which receptors to target and determine the most promising combination of antibodies to induce robust clinical outcomes, precise knowledge of receptor expression on immune cells in general and on tumor-infiltrating lymphocyte (TIL) subsets is essential. In this study, we observed elevated CD96 expression on CD8+ TILs from CC specimens that were irresponsive to PD-1 blockade. The coexpression of CD96 and PD-1 distinguished a subset of terminally exhausted effector CD8+ TILs and indicated that the combined blockade of CD96 and PD-1 could be applied for CD8+ T cell-mediated tumor control. These findings suggest that a therapeutic strategy based on the cotargeting of CD96 and PD-1 in CC is tractable.

MATERIALS AND METHODS

Patients and specimens

CC tumor resection specimens and peripheral venous blood were obtained from the Tissue Bank of Obstetrics and Gynecology Hospital, Fudan University. A total of 43 patients pathologically diagnosed with CC at the Obstetrics and Gynecology Hospital of Fudan University from December 2019 to November 2021 were enrolled in this study. At least two hospital pathologists histologically assessed the tumor specimens. All samples were anonymously coded as P1–P43. Among these patients, paired blood and peritumorous (PT) and intratumoral (IT) tissues were collected from P17, P21, P23, P25, P30–P42; paired blood and IT tissues were collected from P19; and paired PT and IT tissues were collected from P18. For the rest of patients, IT tissues were collected. The details of all patients are provided in online supplemental table 1.

Assay methods

The experimental procedures of ex vivo treatment assay with human specimens and in vivo treatment experiment with tumor-bearing mouse are listed in online supporting information. The details methods of flow cytometry and immunohistochemistry were also listed in the supporting information. All antibodies used in flow cytometry are listed in online supplemental table S2. The strategy for identifying dendritic cells (DCs), monocytes and CD8+ T cells is shown in online supplemental figure 1.

The Cancer Genome Atlas (TCGA) bioinformatics analysis

Single-cell data were generated from eight CC samples by 10× Genomics with Cell Ranger, which processes chromium single-cell RNA-seq outputs to align reads and generate feature-barcode unique molecular identifier matrices versus cells. After quality control and data processing, 1758 CD96–CD8+ T cells and 3498 CD96+CD8+ T cells were included in the analysis. To define signatures for CD96– or CD96+ CD8+ T cells, differential expressed gene (DEG) analysis was carried out based on a log fold change of >0.25, pct of >0.1, and p value of <0.05. The DEGs passing the criteria are shown in online supplemental table 3. Gene expression and matched survival data from the TCGA cervical squamous cell carcinoma and endocervical adenocarcinoma (CESC) dataset were downloaded from the TCGA Data Portal. The gene expression data were normalized by taking the log2(FPKM+1) formula. The signature score of CD96+CD8+ T cell or CD96–CD8+ T cell was calculated as the geomean of normalized signature gene expression.

Statistical analysis

Statistical analyses were performed using IBM SPSS Statistics V24.0 software. The Mann-Whitney U test was used to compare two groups, and the Kruskal-Wallis test was used to compare multiple groups. Additionally, the Wilcoxon matched-pairs signed-rank test and the Friedman test were used for paired comparisons of two or multiple groups. For analysis of OS, Kaplan-Meier estimates and the log-rank test were used. Differences with p values of <0.05 were considered statistically significant.

RESULTS

Patients with CC insensitive to PD-1 blockade exhibit higher CD96 expression on CD8+ TILs

To model the patient response to anti-PD-1 treatment, a patient-derived tumor ex vivo treatment assay (figure 1A) was used according to previous studies.[11 12] We isolated single-cell suspensions from 14 surgically resected CC tumors and treated the tumor suspensions for 24 hours in the presence of pembrolizumab or the IgG control. After ex vivo treatment, functional markers of cytotoxic T lymphocytes (CTLs) and annexin V/PI staining of CD45– cells were assessed by flow cytometry (online supplemental figure 2A). The CTL response was calculated according to the geomean index of the proportion of cells positive for proliferation marker (Ki67), effector cytokines (interleukin (IL)-2, interferon gamma (IFN-γ), tumor necrosis factor alpha (TNF-α)) and cytolytic markers (CD107a, granzyme B (GZMB), and perforin-1 (PRF1)) among CD8+ TILs. Tumor apoptosis was represented as the sum of annexin V+ or PI+ CD45 cells. Specimens that exhibited more than 1.5-fold increase in both the CTL response and tumor apoptosis after

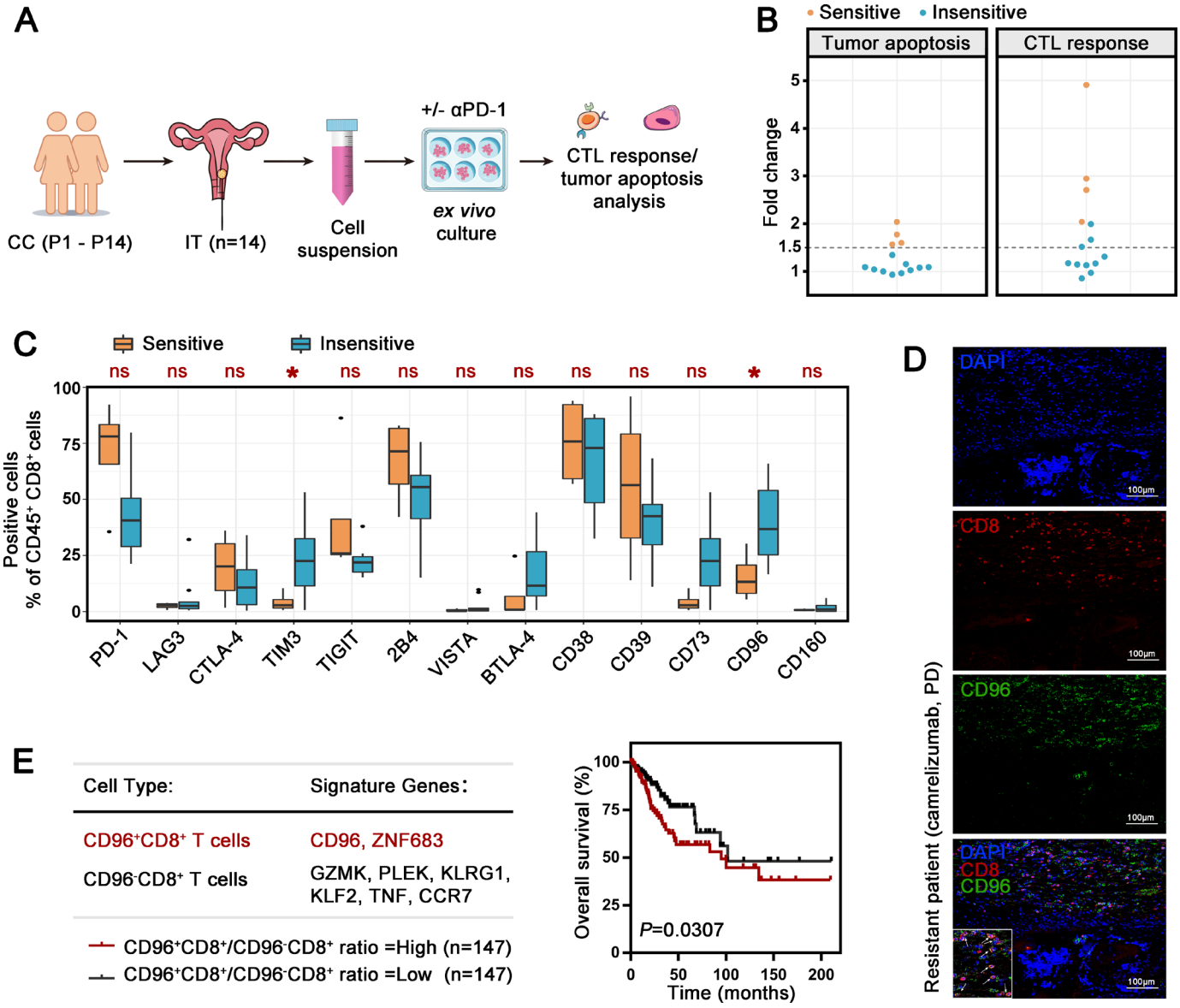

Figure 1 Association of iR expression on CD8+ TILs with the pembrolizumab response in patients with CC. (A) Schematic ex vivo treatment strategy for figure 1. Single-cell suspensions from 14 CC specimens (P1–P14) were incubated ex vivo for 24 hours with αPD-1 or isotype IgG control before flow cytometry analysis to assess tumor apoptosis and the CTL response. (B) Fold changes in tumor apoptosis and CTL response in the presence of αPD-1 compared with isotype IgG control. Sensitivity and insensitivity were distinguished with a fold change cut-off of 1.5 in both analyses. (C) Percentages of different iR-positive cells within CD45+CD8+ TILs in 4 αPD-1-sensitive specimens and 10 αPD-1-insensitive specimens. The data are shown as iR expression before αPD-1 treatment. (D) Representative immunofluorescence images of CD8+ and CD96+ cells in the CC specimen from a patient resistant to camrelizumab (progression disease). Original magnifications: ×200. (E) Signature genes identifying CD96+CD8+ T cells and CD96−CD8+ T cells (left). Kaplan-Meier plot of the overall survival of patients with cervical squamous cell carcinoma and endocervical adenocarcinoma (n=294) based on the CD96+CD8+ T cell/CD96−CD8+ T-signature score ratio (right). The data are dichotomized into 'high' (red, n=147) and 'low' (black, n=147) using median value. Experiments were performed independently for each specimen. P values were obtained by the Mann-Whitney U test (C) and log-rank test (E). *P<0.05. αPD-1, antibodies against PD-1; CC, cervical cancer; CTL, cytotoxic T lymphocyte; DAPI, diamidinyl phenyl indole; iR, inhibitory receptor; IT, intratumoral; TIL, tumor-infiltrating lymphocyte; ns, not significant; PD-1, programmed cell death protein 1.

pembrolizumab treatment compared with that in the control group were considered sensitive (figure 1B). In 4 of 14 specimens, pembrolizumab elicited effective checkpoint inhibition. Next, we investigated the expression of multiple checkpoints in the 4 sensitive patients and 11 insensitive patients. T-cell immunoglobulin mucin receptor 3 (TIM-3) and CD96 were significantly elevated on CD8+ TILs from insensitive CC specimens, while other checkpoints (lymphocyte activation gene 3 protein (LAG-3), cytotoxic T-lymphocyte protein 4 (CTLA-4), TIGIT, 2B4, V-type immunoglobulin domain-containing suppressor of T-cell activation (VISTA), BTLA-4, CD38,

CD39, CD73, and CD160) did not differ between the two groups (figure 1C). As a classic checkpoint, TIM-3 has been explored in detail in multiple studies. The novel checkpoint CD96, which was highly expressed in CC specimens, attracted our interest (online supplemental figure 2B). We collected the primary surgical tumor sample from a patient resistant (response: progression disease (RECV.1.1]) to camrelizumab, a PD-1 inhibitor, in treatment after postoperative recurrence. Using immunofluorescence, we observed widely CD96 expression on CD8+ TILs (positive ratio 76.8%, figure 1D).

To determine the role of CD96+CD8+ T-cell abundance in CC, we used our single-cell RNA-seq data (unpublished data) to identify signature genes of CD96+CD8+ T cells and CD96−CD8+ T cells (online supplemental figure 2C and figure 1E). The specific expression of identified signature genes on CD8+ T-cell population was further confirmed by flow cytometry using three samples (online supplemental figure 2D,E). Using the CESC dataset from the public TCGA database,[13] the signature score ratio of CD96+CD8+ T cells versus CD96−CD8+ T cells was significantly associated with poor OS (figure 1E). These data suggest the crucial role of CD96+CD8+ T cells in the tumor evasion in CC.

CD96 is upregulated and coexpressed with PD-1 on IT CD8+ cells

We collected an additional 15 IT specimens, 5 paired PT specimens and five paired blood samples to further explore the role of CD96 in CC and PD-1 blockade. CD8+ T cells from the blood samples, PT samples and half of the bisected IT samples were analyzed by flow cytometry (online supplemental figure 3A). We found extremely low expression of both PD-1 and CD96 on CD8+ T cells in blood (figure 2A). Compared with that in the PT sample, the expression of CD96 and PD-1 was significantly higher on IT CD8+ T cells (figure 2A). The frequency of CD96+ cells among CD8+ TILs was not correlated with the clinical stage (online supplemental figure 4A). The difference among the different histological types was likely due to the small sample size used in the study (online supplemental figure 4A). Interestingly, CD8+ T cells that expressed CD96 often coexpressed PD-1 in both IT and PT tissues (figure 2B, online supplemental figure 4B). IT samples were evaluated for PD-1 blockade response in the same manner as that described for figure 1B (online supplemental figure 3B); 3 samples were identified as sensitive, and 12 samples were insensitive. In combination with the 14 samples in figure 1, we further confirmed

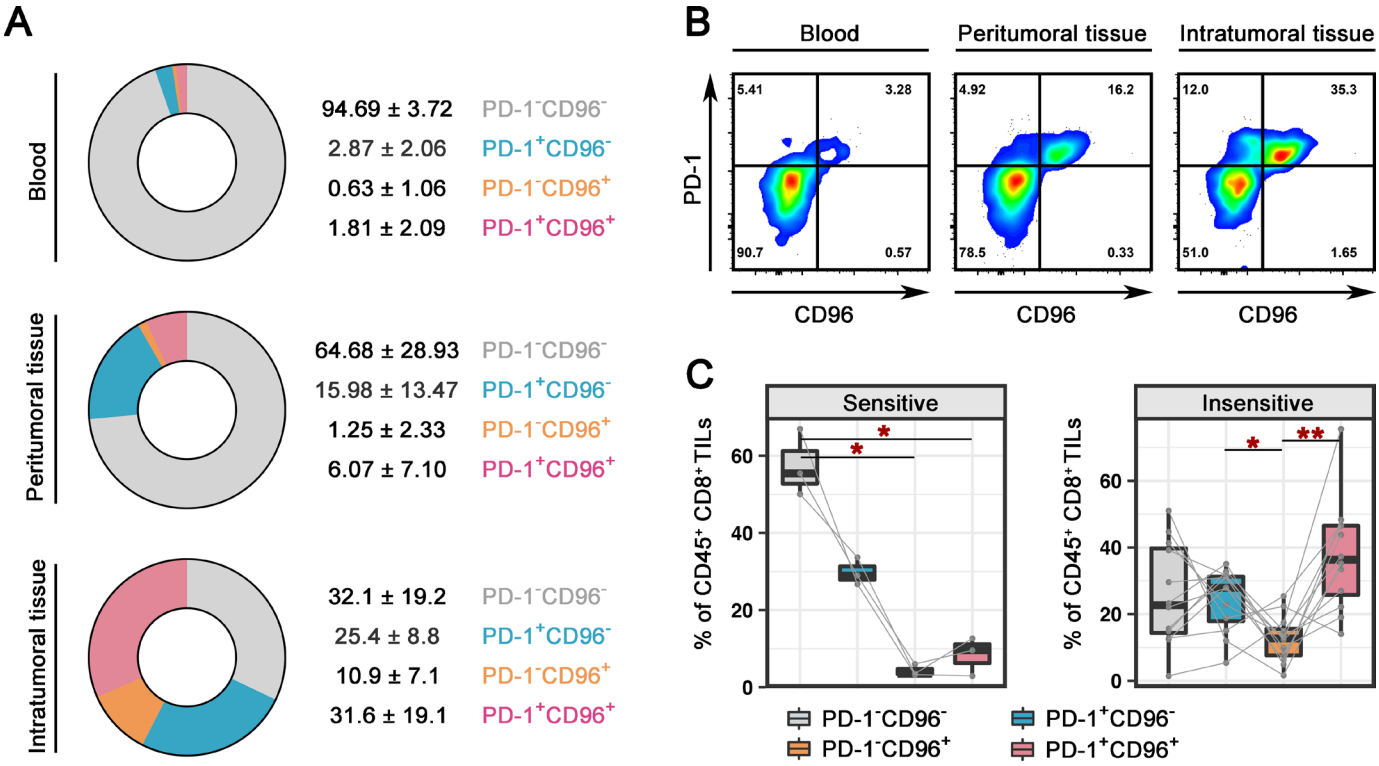

Figure 2 Coexpression of CD96 and PD-1 on CD8+ TILs. (A) Pie charts showing the proportions of PD-1-CD96−, PD-1+CD96−, PD-1-CD96+, and PD-1+CD96+ cells among CD45+CD8+ T cells in blood (top, n=5), PT (middle, n=5) and IT samples (bottom, n=15) from patients with CC. (B) Representative dot plots showing the CD96 and PD-1 expressions on CD45+CD8+ T cells in paired blood (left), PT (middle) and IT (right) samples. (C) Percentages of PD-1−CD96−, PD-1+CD96−, PD-1−CD96+, and PD-1+CD96+ cells among CD45+CD8+ TILs from CC samples that were sensitive (n=3, left) and insensitive (n=12, right) to αPD-1. The data are shown as iR expression before αPD-1 treatment. P values were obtained by the Friedman test (D). *P<0.05, **P<0.01. αPD-1, antibodies against PD-1; CC, cervical cancer; iR, inhibitory receptor; IT, intratumoral; PD-1, programmed cell death protein 1; PT, peritumorous; TIL, tumor-infiltrating lymphocyte.

the significant upregulation of CD96 in PD-1-insensitive specimens (online supplemental figure 4C). Of note, CD8+ TILs that were positive for both PD-1 and CD96 (37.44±16.6) were far more frequent than CD8+ TILs that were positive for only CD96 (12.52±7.0) among patients who were insensitive for pembrolizumab (figure 2C, online supplemental figure 4D). Although the expression of CD96 on the CD8+ TILs of sensitive patients was lower than that on those of insensitive patients, the percentage of CD96+PD-1+ cells was twofold higher than percentage of CD96–PD-1+ cells (figure 2C, online supplemental figure 4D). Collectively, our results demonstrate that CD96 expression is upregulated on CD8+ TILs from patients with CC and that the majority of CD8+ TILs coexpress CD96 and PD-1.

CD96+PD-1+CD8+ TILs exhibit a terminally exhausted effector phenotype

To investigate the differentiation status of CD96+PD-1+CD8+ TILs, CC specimens (P15–P29) were further evaluated for CD45RA and CCR7 expression. T cells can be divided into naïve T cells, central memory T cells, effector memory T (Tem) cells, and terminally differentiated effector memory T (TEMRA) cells according to the expression of CD45RA and CCR7. A higher percentage of CD96+PD-1+CD8+ TILs (compared with those CD96+PD-1-, CD96-PD-1+, and CD96-PD-1- CD8+ TILs) showed TEMRA features with limited memory potential (figure 3A).

We further examined the expression pattern of TIM-3, which is reported to be an inhibitory receptor (iR) together with PD-1 expressed on exhausted CD8+ TILs.[14] The double-negative CD8+ TILs scarcely expressed TIM-3; CD96- or PD-1- positive CD8+ TILs exhibited upregulated TIM-3 expression; and CD96+PD-1+CD8+ TILs had the highest proportion of TIM-3+ cells, suggesting that CD96 and/or PD-1-positive CD8+ TILs have an exhausted phenotype (figure 3B).

Next, we examined the expression of the transcription factors Eomes and TCF-1, which contribute to the programming and maintenance of the exhausted phenotype.[15–17] The proportion of Eomes-positive cells was not significantly different in CD8+ TIL subgroups divided according to CD96 and PD-1 (figure 3C). Notably, CD96 or PD-1 single-positive cells exhibited marked upregulation of TCF-1, a transcription factor involved in sustaining the proliferative capacity of exhausted T cells (figure 3C),[18] indicating that CD96–PD-1+CD8+ TILs display 'stem-like' precursor exhausted T (Tpex) cell features.[19] In contrast, double-negative and double-positive cells expressed low amounts of TCF-1. This feature aligned with the high

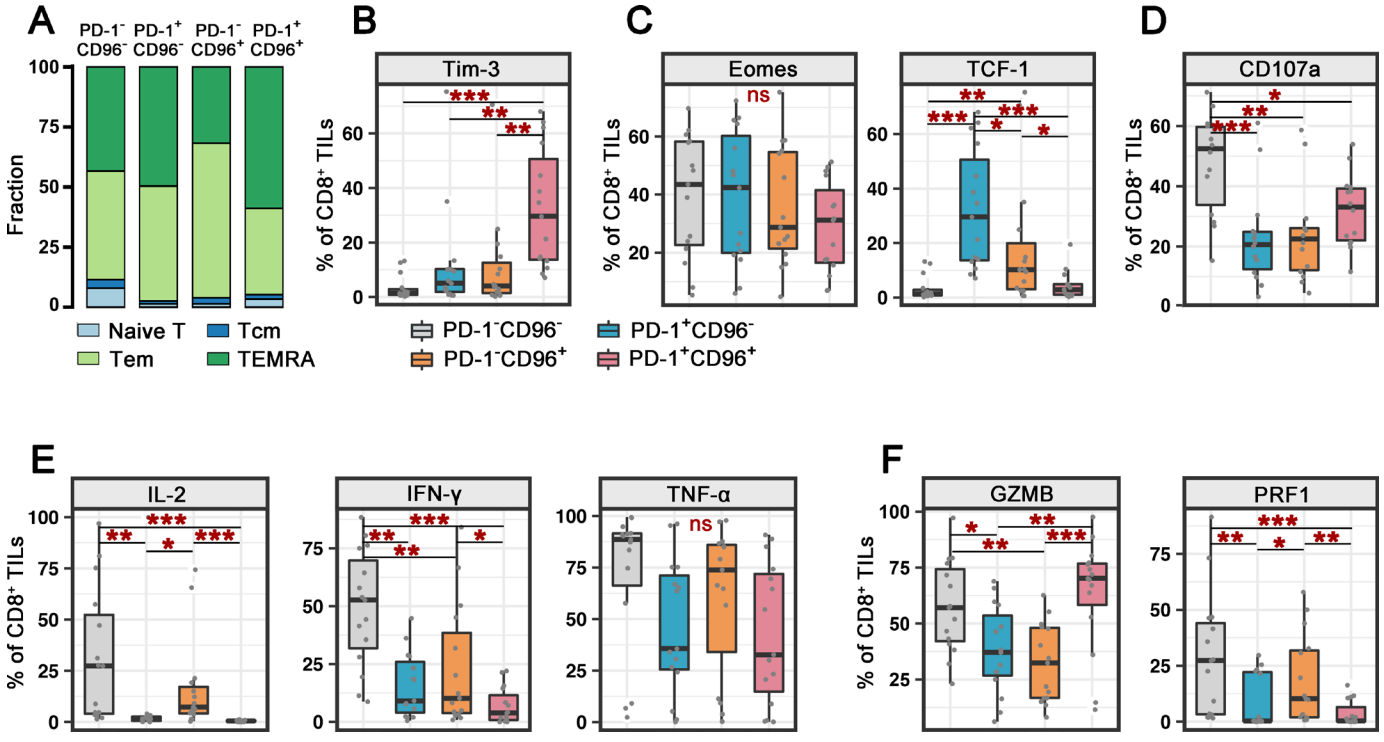

Figure 3 Characterization of memory, transcription, and functional molecules on CD96+PD-1+CD8+ TILs. (A) Proportion of naïve T, Tcm, Tem, and TEMRA cells among PD-1–CD96–, PD-1+CD96–, PD-1–CD96+, and PD-1+CD96+CD8+ TILs from patients with CC (n=15). (B–F) Percentages of exhausted cell marker (B), transcription factor (C), degranulation marker (D), effector cytokine (E) or cytolytic protein (F) expression on PD-1–CD96–, PD-1+CD96–PD-1–D96+, and PD-1+CD96+CD8+ TILs from patients with CC (n=15). P values were obtained by the Kruskal–Wallis test. *P<0.05, **P<0.01, ***P<0.001. CC, cervical cancer; IFN-γ, interferon gamma; IL, interleukin; ns, not significant; PD-1, programmed cell death protein 1; Tcm, central memory T; Tem, effector memory T; TEMRA, terminally differentiated effector memory T; TIL, tumor-infiltrating lymphocyte ; TNF-α, tumor necrosis factor alpha.

proportion of TEMRA cells, indicating that CD96+PD-1+CD8+ TILs are terminally differentiated cells lacking self-renewal ability.

We then characterized the functional profiles of CD8+ TILs with regard to differential CD96 and PD-1 expression. The degranulation marker CD107a on CD8+ T cells was most highly expressed by CD96–PD-1–CD8+ TILs and was significantly reduced in single-positive and double-positive cells (figure 3D). Similarly, the proportion of cells producing effector cytokines (IL-2, IFN-γ, and TNF-α) was highest for CD96–PD-1–CD8+ TILs, and the percentages of IL-2+, IFN-γ+ and TNF-α+ cells were decreased and similar in the CD96+ and/or PD-1+ counterparts (figure 3E). In addition, compared with the double-negative cells, the CD96+PD-1− and CD96–PD-1+CD8+ TILs showed reduced expression of the cytolytic proteins GZMB and PRF1 (figure 3F). Interestingly, the CD96 +PD-1+CD8+ TILs exhibited lower PRF1 expression but significantly higher GZMB expression than single positive cells (figure 3F). We compared the features of CD96 +PD-1+CD8+TILs in PD-1-sensitive and PD-1-insensitive patients, and the results revealed no difference in the expression levels of the aforementioned markers (online supplemental figure 5). These results suggest the existence of an inherent terminally exhausted effector phenotype of CD96+PD-1+CD8+ TILs.

Taken together, our results suggest that in patients with CC, CD96+PD-1+CD8+ TILs exhibit the features of the terminal exhausted effector phenotype, while CD96–PD-1+CD8+ TILs have a more precursor exhausted-like phenotype.

CD96 blockade enhances PD-1 blockade to unleash CD8+ TIL function ex vivo

We then sought to assess whether CD96 blockade in conjunction with the blockade of PD-1 could restore the function of CD8+ TILs from patients with CC to a greater extent than PD-1 blockade alone. Using the other half of the bisected IT specimens from P15–P29, we established a short-term ex vivo culture system similar to that indicated in figure 1A, via which tumor single cells were treated for 24 hours in the presence of blocking antibodies against PD-1 (αPD-1) and/or antibodies against CD96 (αCD96) or an irrelevant isotype control antibody (online supplemental figure 3B). To more intuitively show the PD-1 response, 3 sensitive samples are shown as dots without border, and 12 insensitive samples are shown as dots with black borders. Ex vivo stimulation assays revealed that the apoptotic ratio of CD45− cells was modestly increased in the single PD-blockade and single CD96-blockade groups compared with the control group. Dual blockade of PD-1 and CD96 further increased the apoptosis of CD45− cells by 1.9-fold compared with that in the control group (figure 4A, (online supplemental figure 6A). In 9 of the 15 patients, we observed a more than 1.5-fold increase in tumor apoptosis compared with that in the control group.

We next assessed whether CD96 blockade promoted the antitumor response of CD8+ TILs by detecting the proliferation, cytokine production, and degranulation of CD8+ TILs. For each functional marker, we calculated the percentages of marker-positive cells and the ratio of the fold change versus the control group. As shown for 15 patients, dual blockade further increased the percentages of IL-2 expression among CD8+ TILs compared with PD-1 blockade (online supplemental figure 6B), but the increase was not significant in fold change (figure 4B). Moreover, a prominent increase in IFN-γ+CD8+ TIL numbers was observed in the dual PD-1/CD96-blockade group compared with the single-blockade group (figure 4B and online supplemental figure 6B). Neither the blockade of PD-1 or CD96 alone nor the dual blockade affected the mean TNF-α cytokine level (figure 4B and online supplemental figure 6B). Similarly, dual blockade promoted the proliferation of CD8+ TILs, as indicated by the significantly elevated Ki67+ cell proportion compared with that in the control and single-blockade groups (figure 4C, online supplemental figure 6C). Moreover, blockade of PD-1 or CD96 alone resulted in a more than 1.5-fold increase in cytotoxic markers (CD107a, GZMB and PRF1) in only a small proportion of specimens. In contrast, blockade of PD-1 together with CD96 resulted in a significantly higher percentage of cytotoxic CD8+ TILs than the single blockade, and these increases were observed in more specimens than those treated with the single blockade (figure 4D, online supplemental figure 6D). Furthermore, we classified the samples based on the PD-1 blockade response and compared the effect of dual blockade therapy. For insensitive samples, both tumor apoptosis and the CTL response were greatly induced after dual blockade (online supplemental figure 6E). For sensitive samples, there was no significant difference between the dual and single blockades, and tumor apoptosis was increased in the dual blockade group by 1.5-fold to 2.0-fold compared with that in the single PD-1-blockade group for two of three samples (online supplemental figure 6E). Collectively, our findings show that CD96 blockade facilitates stronger antitumor CD8+ TIL function when combined with PD-1 blockade.

Finally, the expression of PD-1 and CD96 was assessed on PD-1 and CD96 blockade after 24 hours of culture as described previously. The expression of PD-1 on CD8+ TILs was not affected by CD96 blockade, suggesting that the receptor was not modulated after targeting CD96 (figure 4E). In contrast, we observed a clear upregulation of CD96 after PD-1 blockade (vs IgG control) on CD8+ TILs from most of the tested patients (figure 4E, online supplemental figure 6F). The expression of PD-1 and CD96 was not affected by autoblockade in the 24-hour short-term culture (online supplemental figure 6G). These results may indicate a PD-1-resistant phenotype of CD8+ TILs during the blockade of PD-1 and provide a rationale for the PD-1 and CD96 blockades in combination.

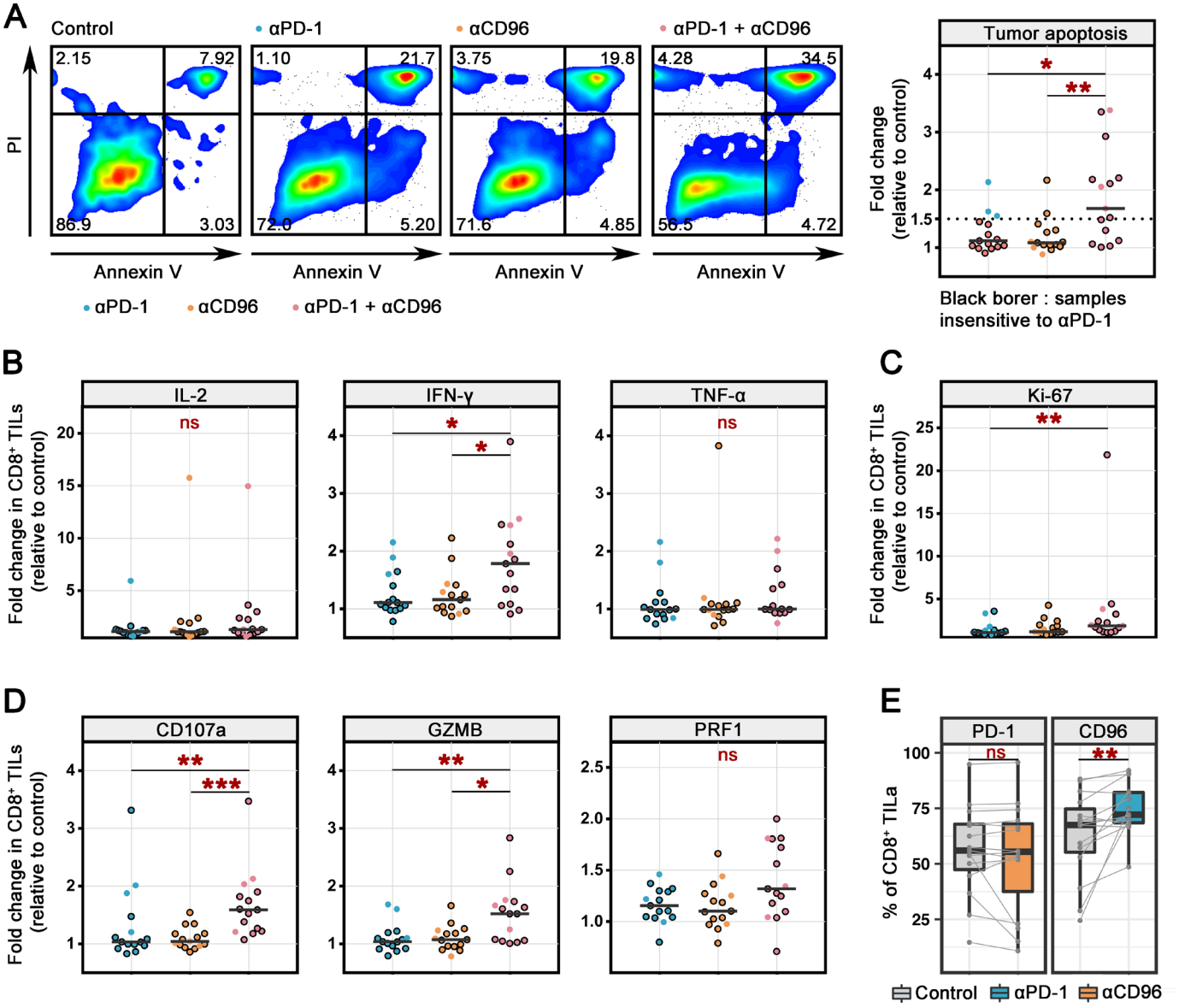

Figure 4 Recovery of CD8+ TIL function following PD-1 and CD96 blockade treatment ex vivo. (A) Representative dot plots showing the apoptosis of tumor cells from 1 CC specimen after treatment with αPD-1, and/or αCD96 or the IgG control for 24 hours (left). The fold change was calculated as the ratio of the treatment group value compared with the control group value (n=15) (right). The PD-1 blockade-insensitive samples are shown with a black border. (B–D) Fold changes in the percentages of effector cytokine (B), proliferation marker (C), and cytolytic marker (D) expression on CD45+CD8+ TILs after treatment with αPD-1 and/or αCD96 or the IgG control for 24 hours (n=15). The PD-1 blockade-insensitive samples are shown with a black border. (E). Percentages of PD-1-positive (left) or CD96-positive (right) cells among CD45+CD8+ TILs after treatment with αCD96, αPD-1 or IgG control for 24 hours (n=15). Experiments were performed independently for each specimen. Values were obtained by the Kruskal-Wallis test (A–D) and the Wilcoxon matched-pairs signed-rank test (E). *P<0.05, **P<0.01, ***P<0.001. αCD96, antibodies against CD96; αPD-1, antibodies against PD-1; CC, cervical cancer; IFN-γ, interferon gamma; IL, interleukin; ns, not significant; ns, not significant; PD-1, programmed cell death protein 1; TIL, tumor-infiltrating lymphocyte; TNF-α, tumor necrosis factor alpha.

Balance between CD226/CD96/TIGIT signaling is broken in patients with CC

CD226, CD96 and TIGIT together form a pathway shaping the immune response in which CD96 and TIGIT deliver inhibitory signals, whereas CD226 delivers activating signals.[20] We thus hypothesized that immune balance may be disrupted between the two signaling pathways to decide the net activation or inhibition of CD8+ TILs. To address this, we analyzed the expression of CD226, CD96 and TIGIT on CD8+ T cells in blood, tumor and PT samples (online supplemental figure 3C). In the blood and tumor PT samples from patients with CC, CD226+ cells accounted for the major proportion of CD8+ T cells, while CD96+ and TIGIT+CD8+ T cells were present at low frequencies in the PT samples and were rarely observed in the blood (figure 5A). In tumors, the proportion of the CD96+ and TIGIT+ subset was substantially increased, and that of the CD226+ subset

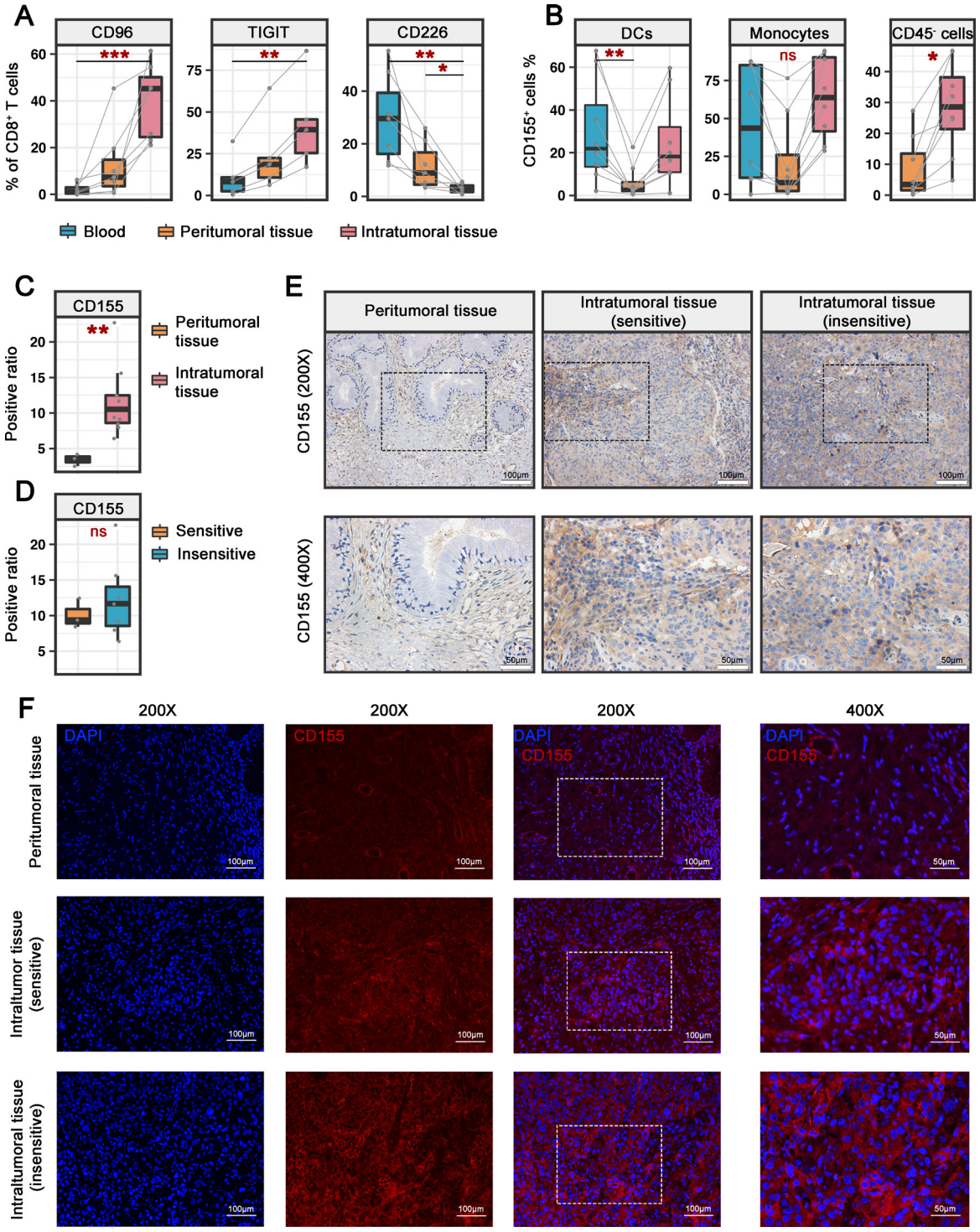

Figure 5 The imbalance of CD226/CD96/TIGIT signals in patients with CC. (A) Percentages of CD96-positive (n=7), TIGIT-positive (n=5) and CD226-positive (n=7) cells among CD8+ T cells from paired blood, PT and IT specimens from patients with CC. (B) Percentages of CD155+ cells among DCs and monocytes from paired blood, PT and IT specimens from patients with CC (n=8) (left, middle). Percentages of CD155+ cells among CD45– cells from paired PT and IT specimens from patients with CC (n=8) (right). (C) Quantification of the CD155+ ratio per field for PT (n=3) and IT (n=10) specimens. Three fields of each slide were randomly picked. (D) Quantification of the CD155+ ratio per field for αPD-1-sensitive IT (n=3) and αPD-1-insensitive IT (n=7) specimens. Three fields of each slide were randomly picked. (E) Representative immunohistochemistry images showing CD155+ cells in PT, αPD-1-sensitive IT, and αPD-1-insensitive IT specimens. Original magnifications: ×200 (upper) and ×400 (bottom). (F) Representative immunofluorescence images showing CD155+ cells in PT, αPD-1-sensitive IT, and αPD-1-insensitive IT specimens. Original magnifications: ×200 (left) and ×400 (right). Experiments were performed independently for each specimen. P values were obtained by the Friedman test (A,B, left and middle), Wilcoxon matched-pairs signed-ranks test (B, right) and Mann-Whitney U test (C,D). *P<0.05, **P<0.01, ***P<0.001. DC, dendritic cell; IT, intratumoral; ns, not significant; PD-1, programmed cell death protein 1; PT, peritumorous.

was decreased in CD8+ TILs (figure 5A), indicating that CD226+CD8+ T cells were potentially in transition to CD96+ and TIGIT+CD8+ T cells under the influence of the tumor microenvironment.

Both CD96 and TIGIT bind the nectin-like protein CD155 with CD226 but deliver opposite signals. We thus evaluated the expression of CD155 as described by online supplemental figure 3C. CD155 was expressed by high proportions of DCs and monocytes circulating in peripheral blood (figure 5B). For tissue-infiltrated antigen presenting cells (APCs), the percentage of CD155+ cells was low in PT but dramatically increased in tumors (figure 5B). Of note, a certain proportion of non-immune cells also expressed CD155 at high levels in tumors (figure 5B). As further assessed by immunohistochemistry and immunofluorescence, we confirmed that CD155 was widely expressed in IT tissue but weakly expressed in PT tissue (figure 5C, E and F). A comparison of IT specimens that were sensitive and insensitive to αPD-1 (evaluated in figure 4) revealed that CD155 expression did not differ between the groups (figure 5D, E and F). In addition to CD155, CD96 also binds to CD111, while CD226 and TIGIT bind to CD112. We observed markedly high levels of both ligands were observed in tumors compared with adjacent tissue (online supplemental figure 7A,C and D). The ligands for CD226/CD96/TIGIT were strikingly upregulated in tumor tissues regardless of the αPD-1 response (online supplemental figure 7B–D), suggesting a critical role of the CD96 immunoregulatory pathway in regulating the function of CD8+ TILs in CC. Collectively, our findings show an imbalance of CD226/CD96/TIGIT signals in CD8+ TILs that may contribute to the negative immunoregulatory effects of CD96 in the context of CC.

CD96 blockade enhances the therapeutic activity of PD-1 blockade in combination therapy

To explore the effect of CD96 blockade on tumor progression in vivo, the TC-1 tumor-bearing C57BL/6 mouse model was used (figure 6A). Intraperitoneal infusion of either αCD96 (clone 3.3, 200 µg/mouse) or αPD-1 (clone RMP1-14, 200 µg/mouse) two times per week significantly delayed tumor growth (figure 6B) and prolonged the survival of tumor-bearing mice (figure 6C). Moreover, treatment with a combination of antibodies against CD96 and PD-1 enhanced the tumor growth control effect compared with that achieved with a single blockade (figure 6B,C), and complete remission was observed in one tumor-bearing mouse. Ki67 staining of CD45− cells verified the tumor inhibition activity mediated by αCD96 or αPD-1, and the synergistic action of the combination therapy (figure 6D).

In a mouse model, we observed marked upregulation of CD96 on the CD8+ TILs of mice treated with PD-1 blockade but not on those of mice treated with CD96 blockade or the two blockades in combination. In addition, the PD-1 and CD96 blockades alone did not affect the level of PD-1 on CD8+ TILs, but dual blockade significantly downregulated PD-1 expression (figure 6E). These results support the clinical targeting of PD-1 together with CD96 blockade to achieve synergistic effects.

Based on the relationship among CD96, PD-1 and the exhausted phenotype of T cells, we next investigated the effects of the CD96 and PD-1 blockades on the effector function of CD8+ TILs in a tumor-bearing mouse model. We analyzed the percentages of CD8+ TILs that produced effector cytokines or cytolytic proteins. Similar to the ex vivo model, the expression of CD107a and PRF1 in CD8+ TILs was increased after PD-1 or CD96 blockade compared with that in the control group, and the stimulation effect was further enhanced by dual-blockade treatment (figure 6F and online supplemental figure 8). IFN-γ, GZMB and TNF-α, the levels of which were extremely low or high at baseline, tended to increase after dual-blockade treatment, but the difference did not reach statistical significance (figure 6F, online supplemental figure 8).

Therefore, in addition to curing mice of their implanted tumors, blocking CD96 in combination with PD-1 promoted a durable protective antitumor CD8+ T-cell response in a preclinical mouse model.

DISCUSSION

ICB therapy targeting PD-1/PD-L1 has induced significant clinical responses in a subset of patients with cancer[21]; however, various tumor cell-intrinsic and tumor-extrinsic mechanisms have been implicated in therapeutic resistance, and most patients with CC still do not benefit from this treatment option.[8 22] In our study, we aimed to understand the molecular mechanisms underlying immunotherapy resistance and to identify a new promising iR candidate for combined immune checkpoint therapy with PD-1 blockade in patients with CC. Using an ex vivo treatment assay model, we detected significant CD96 upregulation on CD8+ TILs from patients with CC who did not respond to PD-1 blockade, indicating the role of CD96 in PD-1 innate resistance in patients with CC.

The iRs CD96 and TIGIT, together with the costimulatory molecule CD226, comprise a critical regulatory system for lymphocyte activity and antitumor immunity.[23 24] They share the common ligand CD155, and the balance between three receptors may fine-tune the immune response to tumors.[25] Previous studies have demonstrated that CD96 is an intrinsic checkpoint on NK cells that regulates NK cell effector function and metastasis in the tumor microenvironment.[20 25] Additionally, CD96 is expressed on CD8+ T cells in mouse and human tumors (colorectal cancers and metastatic melanoma), and blockade of CD96 either as a monotherapy or in combination with blockade of TIGIT or PD-1 leads to enhanced antitumor immunity in a mouse model.[26] However, there are few relevant studies, and whether CD96 is intrinsically functional as an iR on CD8+ TILs is not yet clear, especially in the context of CC. Here, we detected increased CD96 expression on IT CD8+ TILs compared with PT CD8+ T cells, which was consistent with reports on other human tumors,[26] and we observed very low expression

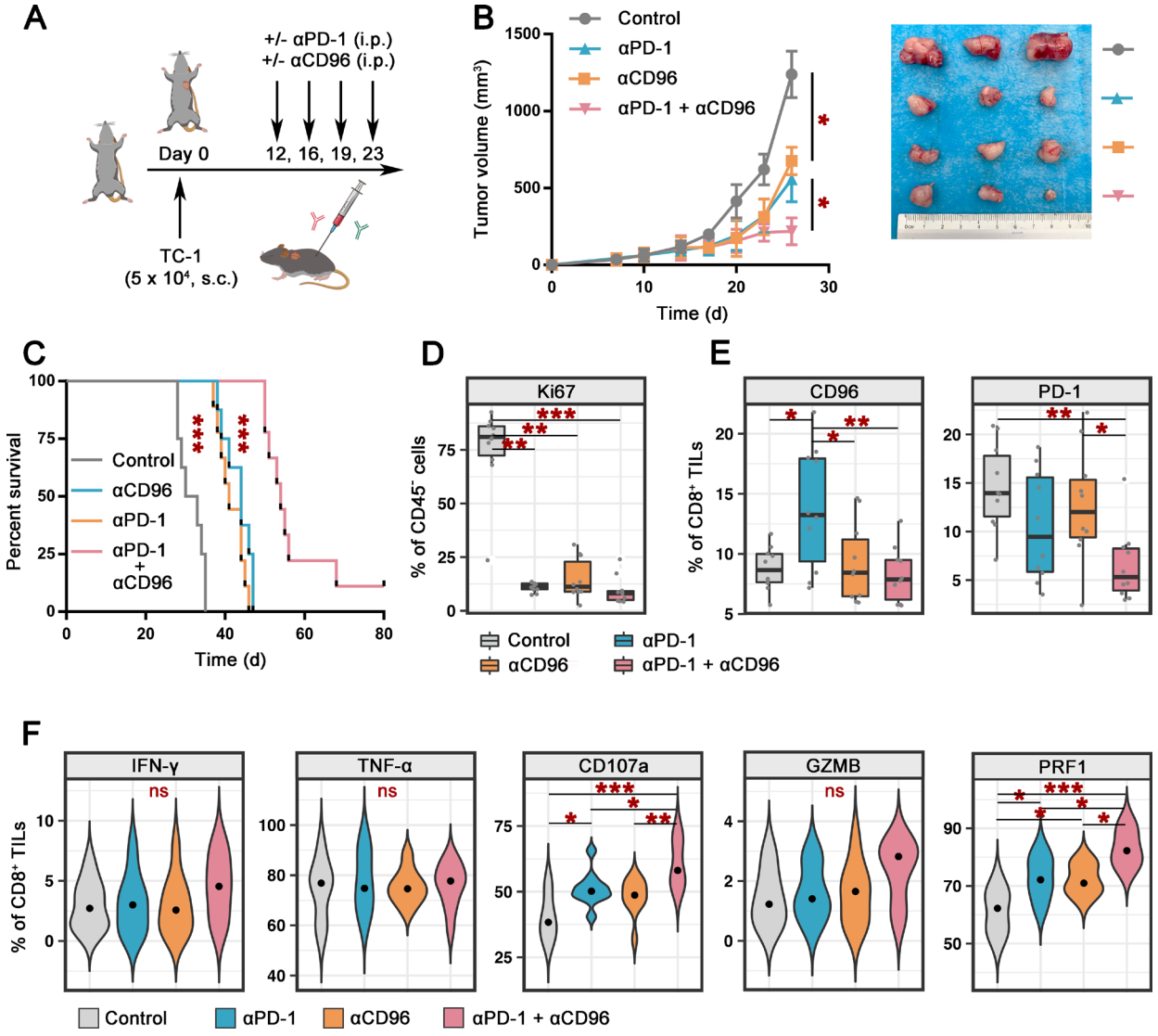

Figure 6 Combined CD96 and PD-1 blockade promotes antitumor immunity in TC-1 tumor-bearing C57BL/6 mice. (A). Schematic representation of the experimental strategy. C57BL/6 mice were given intraperitoneal injections of αPD-1 (clone RMP1-14) and/or αCD96 (clone 3.3) or the IgG control on days 12, 16, 19, and 23 after the injection of 5×10^4 TC-1 tumor cells subcutaneously on day 0 (n=10 for each group). (B) Tumor size in mice treated as described in A (n=10 for each group) at various time points after the challenge (left). Representative photos of tumors in each group on day 26 (right). (C) Survival of mice treated as described in A (n=9 for αPD-1 and the control group, n=10 for αCD96 and the combination group). The survival of the mice was determined by denoting the last day of ethical tumor size measurement as the time of sacrifice. (D) Percentages of Ki67-positive cells within CD45– cells in the tumors of mice treated as described in A (n=10 for each group). (E) Percentages of CD96+ (left, anti-CD96 clone QA19A37) and PD-1+ (right, anti-PD-1 clone 29F.1A12) cells among CD45+CD8+ TILs from mice treated as described in A (n=10 for each group). (F) Percentages of cells expressing effector cytokines and cytolytic markers among CD45+CD8+ TILs from mice treated as described in A (n=10 for each group). Experiments were performed once for a total of 40 mice. P values were obtained by the Kruskal-Wallis test (B,D–F) and log-rank test (C). *P<0.05, **P<0.01, ***P<0.001. αCD96, antibodies against CD96; αPD-1, antibodies against PD-1; IFN-γ, interferon gamma; ns, not significant; PD-1, programmed cell death protein 1; TIL, tumor-infiltrating lymphocyte; TNF-α, tumor necrosis factor alpha.

in blood samples from patients with CC. We also found a dynamic imbalance among the expression of CD96, TIGIT, and CD226 on CD8+ T cells in peripheral blood and PT and IT specimens and observed abundant CD155 ligand expression on tumor-infiltrating APCs and tumor cells, indicating the dominance of inhibitory signaling in the tumor microenvironment.

In a previous study, CD96 was found to be coexpressed with PD-1 on CD8+ TILs in both mouse and human colorectal cancers and metastatic melanoma.[26] Consistent with this study, our data showed that CD96 was coexpressed in the large majority of PD-1+CD8+ TILs. To further elucidate the role of increased CD96 expression on CD8+ TILs in CC and the functions of CD96 as an intrinsic iR in CD8+ T cells and PD-1 resistance, we analyzed the function and phenotype of CD8+ TILs according to CD96 and PD-1 expression. We found that compared with cells double-negative for PD-1 and CD96,

PD-1+ and/or CD96+ cells were more exhausted and had impaired effector functions, including the secretion of IL-2, TNF-α, and IFN-γ.[14 15] Of note, CD96-PD-1+CD8+ TILs displayed a unique phenotype similar to Tpex cells, characterized by positive TCF-1 expression and negative TIM-3 expression and the cytotoxic molecule GZMB, while CD96+PD-1+CD8+ TILs were terminally exhausted effector cells, characterized by the upregulation of TIM-3 and GZMB expression and the lack of TCF-1 expression.[19 27 28] In the tumor microenvironment, a persistent antigen load continually forces the progressive exhaustion of PD-1+CD8+ TILs from the precursor to terminal state.[17 29] Tpex and Tex cells share the phenotypical and functional characteristics of exhausted T cell, such as elevated iR expression and an impaired cytokine secretion ability, manifested as the the early loss of TNF-α and IL-2 and the later loss of IFN-γ and PRF1.[28 30–32] Tex cells coexpress multiple iRs including TIM-3 and have diminished polyfunctionality but retain their GZMB-based cytolytic potential.[33] Tpex cells exhibit hallmarks of both exhausted and memory cells, display a self-renewing capacity and give rise to exhausted T (Tex) cells.[34] Although PD-1 blockade was initially thought to reinvigorate exhausted T cells, T-cell immunity is only transiently boosted, and T-cell exhaustion is not reversed.[35 36 37] Rather, the antitumor response facilitated by anti-PD-1 arises from a numerical increase in exhausted T cells driven by the proliferative activity of Tpex cells, but the exhausted phenotype is retained by epigenetic enforcement.[19 31 34 37] The large proportion of CD96+PD-1+CD8+Tex cells which that are resistant to PD-1 blockade may contribute to the insensitivity of patients with CC. In this context, novel therapeutic approaches will need to consider how different treatments and strategies elicit TILs in patients with high CD96 expression.

In patients with CC who were not sensitive to PD-1 blockade, CD96 was highly expressed, indicating that a large number of PD-1+CD96+Tex cells had infiltrated the tumor. In addition, we observed an intrinsic phenotypical shift of CD8+ TILs after PD-1 blockade, showing CD96 upregulation, indicating that on stimulation with PD-1 blockade, the subset of PD-1+CD96 Tpex cells may partly transition to PD-1+CD96+ Tex cells, which cannot be further activated by PD-1 blockade. Accordingly, we speculated that dual PD-1/CD96 blockade is a promising strategy for primary PD-1-resistant patients with CC. Moreover, dual PD-1/CD96 blockade can be used to overcome secondary PD-1 resistance by blocking acquired CD96 signals in CD8+TILs.

It is critical to evaluate the efficacy of dual CD96/PD-1 blockade therapy in preclinical tumor models. Thus, we used both a tumor-bearing mouse model and a CC specimen short-term ex vivo treatment model to observe synergistic effects. Overall, we showed that ex vivo treatment with αCD96 and αPD-1 boosted CD8+ TIL proliferation, cytokine production, and degranulation against CC tumor specimens, which was more effective than αPD-1 treatment alone. Dual blockade exhibited a significant antitumor effect on specimens that were insensitive to αPD-1. Although statistical evidence supporting the use of CD96 blockade for patients sensitive to PD-1 blockade was not acquired, which was potentially attributed to our limited sample size, this combination deserves further exploration, as indicated by our ex vivo treatment results. In the future, a prospective clinical study with a large cohort comprehensively assessing clinical benefits, treatment cost, and side effects will be needed to determine whether combination therapy with CD96 blockade is necessary for PD-1 blockade responders. Consistent with data in human specimens, treatment with a combination of CD96 blockade therapies augmented the antitumor efficacy of PD-1 blockade in a tumor-bearing mouse model. This combination therapy was also confirmed to be effective in de novo fibrosarcoma tumors and a CT26 colon carcinoma mouse model.[26] In a B15F10 lung metastasis model, the efficacy of anti-CD96 mAb was more potent than either CTLA-4 or PD-1 blockade.[20] Our TC-1 transplanted tumor model results showed that a single anti-CD96 agent was not inferior to anti-PD-1 at either prolonging survival or promoting CD8+ T cell-mediated tumor inhibition. The possibility of CD96 blockade monotherapy should be further studied in the future. Moreover, long-term immune-related toxicities and autoimmunity were not observed in targeted mice that were deficient for both PD-1 and CD96.[20 38] These data suggest that cotargeting the CD96 and PD-1 pathways can enhance tumor control efficacy and will be of great clinical utility.

In conclusion, our data revealed increased CD96 expression in patients with CC who are not sensitive to PD-1 blockade. CD96 is coexpressed with PD-1 in a large proportion of IT CD8+ T cells. Phenotypical analysis revealed that PD-1-coexpressing and CD96-coexpressing CD8+ TILs exhibited a terminally exhausted effector phenotype, while single-positive cells exhibited a more precursor exhausted-like phenotype. In addition, the balance among CD96/TIGIT/CD226 signals on CD8+ T cells was disrupted in the tumor bed. These results suggest that the CD96 pathway plays an immunoregulatory role in CD8+ T-cell function and PD-1 resistance. Importantly, CD96 blockade enhanced PD-1 blockade by boosting antitumor CD8+ TIL function in preclinical models. The baseline expression of CD96 may be a predictor of PD-1 blockade resistance and a marker for combination therapy. Cotargeting of CD96 and PD-1 may induce greater antitumor immune responses than single-targeted therapies and may pave the way for the future development of CC therapeutics.

Acknowledgements The authors thank AJE (www.AJE.com) for its linguistic assistance during the preparation of this manuscript.

Contributors YW, GL, and KH initiated the project and designed and supervised the research plan. YW, JP, CL, MZ (Mingxing Zhang), MZ (Meng Zhang), and X-LQ performed stimulation experiments under the supervision of JQ. YW, GL and KH wrote the manuscript. YW, CW, JQ, and XQ designed and performed the supplementary experiments. YW, CW, JQ, XQ and GL made significant revisions in language to the manuscript. The order of first authorship was determined by

contribution to project design. All authors edited and approved the manuscript. GL is responsible for the overall content as guarantor.

Funding This project was supported by funding from the National Natural Science Foundation of China (number 81971361, to JQ), the Natural Science Foundation of Shanghai Science and Technology (number 19ZR1406900, to JQ), the Shanghai 'Rising Stars of Medical Talent' Youth Development Program (number AB83030002019004, to JQ), the Clinical Research Plan of SHDC (number SHDC2020CR4087, to JQ), Shanghai Municipal Health Commission (number 202040498, to JQ), the Research and Innovation Project of the Shanghai Municipal Education Commission (number 2019-01-07-00-07-E00050; to KH) and the Clinical Research Plan of SHDC (number SHDC2020CR1045B, to KH), and the National Natural Science Foundation of China (number 81873124, to GL).

Competing interests None declared.

Patient consent for publication Consent obtained directly from patient(s)

Ethics approval All procedures using human tissues conformed to the guidelines of the Declaration of Helsinki and Tokyo for human experimentation, and were approved by the ethics committee of obstetrics and gynecology, Hospital of Fudan University (2019-123). Informed consent was obtained from all subjects prior to inclusion in the study. All studies involving animals were approved by the ethics committee for animal experimentation of Fudan University (201904006Z).

Provenance and peer review Not commissioned; externally peer reviewed.

Data availability statement Data are available upon reasonable request.

ORCID iD

Yumeng Wang http://orcid.org/0000-0001-5772-5924

REFERENCES

1 Siegel RL, Miller KD, Jemal A. Cancer statistics, 2020. *CA Cancer J Clin* 2020;70:7–30.
2 Naga Ch P, Gurram L, Chopra S, *et al*. The management of locally advanced cervical cancer. *Curr Opin Oncol* 2018;30:323–9.
3 Marth C, Landoni F, Mahner S, *et al*. Cervical cancer: ESMO clinical practice guidelines for diagnosis, treatment and follow-up. *Ann Oncol* 2017;28:iv72–83.
4 Institute NC. Cancer STAT facts: cervix uteri cancer, 2020. Available: https://seer.cancer.gov/statfacts/html/cervix.html [Accessed 1 Nov 2020].
5 Chung HC, Ros W, Delord J-P, *et al*. Efficacy and safety of pembrolizumab in previously treated advanced cervical cancer: results from the phase II KEYNOTE-158 study. *J Clin Oncol* 2019;37:1470–8.
6 Haslam A, Prasad V. Estimation of the percentage of US patients with cancer who are eligible for and respond to checkpoint inhibitor immunotherapy drugs. *JAMA Netw Open* 2019;2:e192535.
7 De Felice F, Marchetti C, Palaia I, *et al*. Immune check-point in cervical cancer. *Crit Rev Oncol Hematol* 2018;129:40–3.
8 Liu Y, Wu L, Tong R, *et al*. PD-1/PD-L1 inhibitors in cervical cancer. *Front Pharmacol* 2019;10:65.
9 Santin AD, Deng W, Frumovitz M, *et al*. Phase II evaluation of nivolumab in the treatment of persistent or recurrent cervical cancer (NCT02257528/NRG-GY002). *Gynecol Oncol* 2020;157:161–6.
10 Yoshimura A. *Emerging concepts targeting immune checkpoints in cancer and autoimmunity*. Switzerland: Springer, Cham, 2017.
11 Neal JT, Li X, Zhu J, *et al*. Organoid modeling of the tumor immune microenvironment. *Cell* 2018;175:1972–88.
12 Lin C, He H, Liu H, *et al*. Tumour-associated macrophages-derived CXCL8 determines immune evasion through autonomous PD-L1 expression in gastric cancer. *Gut* 2019;68:1764–73.
13 , Weinstein JN, Collisson EA, *et al*, Cancer Genome Atlas Research Network. The cancer genome atlas pan-cancer analysis project. *Nat Genet* 2013;45:1113–20.
14 Wherry EJ. T cell exhaustion. *Nat Immunol* 2011;12:492–9.
15 Thommen DS, Schumacher TN. T cell dysfunction in cancer. *Cancer Cell* 2018;33:547–62.
16 Philip M, Schietinger A. Heterogeneity and fate choice: T cell exhaustion in cancer and chronic infections. *Curr Opin Immunol* 2019;58:98–103.
17 McLane LM, Abdel-Hakeem MS, Wherry EJ. CD8 T cell exhaustion during chronic viral infection and cancer. *Annu Rev Immunol* 2019;37:457–95.
18 Jeannet G, Boudousquié C, Gardiol N, *et al*. Essential role of the Wnt pathway effector TCF-1 for the establishment of functional CD8 T cell memory. *Proc Natl Acad Sci U S A* 2010;107:9777–82.
19 Siddiqui I, Schaeuble K, Chennupati V, *et al*. Intratumoral TCF1^{+}PD-1^{+}CD8^{+} T cells with stem-like properties promote tumor control in response to vaccination and checkpoint blockade immunotherapy. *Immunity* 2019;50:195–211.
20 Blake SJ, Stannard K, Liu J, *et al*. Suppression of metastases using a new lymphocyte checkpoint target for cancer immunotherapy. *Cancer Discov* 2016;6:446–59.
21 Tumeh PC, Harview CL, Yearley JH, *et al*. PD-1 blockade induces responses by inhibiting adaptive immune resistance. *Nature* 2014;515:568–71.
22 Sharma P, Hu-Lieskovan S, Wargo JA, *et al*. Primary, adaptive, and acquired resistance to cancer immunotherapy. *Cell* 2017;168:707–23.
23 Blake SJ, Dougall WC, Miles JJ, *et al*. Molecular pathways: targeting CD96 and TIGIT for cancer immunotherapy. *Clin Cancer Res* 2016;22:5183–8.
24 Dougall WC, Kurtulus S, Smyth MJ, *et al*. TIGIT and CD96: new checkpoint receptor targets for cancer immunotherapy. *Immunol Rev* 2017;276:112–20.
25 Sun H, Huang Q, Huang M, *et al*. Human CD96 correlates to natural killer cell exhaustion and predicts the prognosis of human hepatocellular carcinoma. *Hepatology* 2019;70:168–83.
26 Mittal D, Lepletier A, Madore J, *et al*. CD96 Is an immune checkpoint that regulates CD8^{+} T-cell antitumor function. *Cancer Immunol Res* 2019;7:559–71.
27 Utzschneider DT, Charmoy M, Chennupati V, *et al*. T cell factor 1-expressing memory-like CD8(+) T cells sustain the immune response to chronic viral infections. *Immunity* 2016;45:415–27.
28 Wu T, Ji Y, Moseman EA, *et al*. The TCF1-Bcl6 axis counteracts type I interferon to repress exhaustion and maintain T cell stemness. *Sci Immunol* 2016;1:aai8593. doi:10.1126/sciimmunol.aai8593
29 Wherry EJ, Blattman JN, Murali-Krishna K, *et al*. Viral persistence alters CD8 T-cell immunodominance and tissue distribution and results in distinct stages of functional impairment. *J Virol* 2003;77:4911–27.
30 He R, Hou S, Liu C, *et al*. Follicular CXCR5- expressing CD8(+) T cells curtail chronic viral infection. *Nature* 2016;537:412–6.
31 Im SJ, Hashimoto M, Gerner MY, *et al*. Defining CD8+ T cells that provide the proliferative burst after PD-1 therapy. *Nature* 2016;537:417–21.
32 Leong YA, Chen Y, Ong HS, *et al*. CXCR5(+) follicular cytotoxic T cells control viral infection in B cell follicles. *Nat Immunol* 2016;17:1187–96.
33 Dolina JS, Van Braeckel-Budimir N, Thomas GD, *et al*. CD8(+) T cell exhaustion in cancer. *Front Immunol* 2021;12:715234–34.
34 Kallies A, Zehn D, Utzschneider DT. Precursor exhausted T cells: key to successful immunotherapy? *Nat Rev Immunol* 2020;20:128–36.
35 Pauken KE, Sammons MA, Odorizzi PM, *et al*. Epigenetic stability of exhausted T cells limits durability of reinvigoration by PD-1 blockade. *Science* 2016;354:1160–5.
36 Barber DL, Wherry EJ, Masopust D, *et al*. Restoring function in exhausted CD8 T cells during chronic viral infection. *Nature* 2006;439:682–7.
37 Miller BC, Sen DR, Al Abosy R, *et al*. Subsets of exhausted CD8^{+} T cells differentially mediate tumor control and respond to checkpoint blockade. *Nat Immunol* 2019;20:326–36.
38 Harjunpää H, Blake SJ, Ahern E, *et al*. Deficiency of host CD96 and PD-1 or TIGIT enhances tumor immunity without significantly compromising immune homeostasis. *Oncoimmunology* 2018;7:e1445949.